




Cite this: *Dalton Trans.*, 2024, **53**, 14258

2-Phenylbenzothiazolyl iridium complexes as inhibitors and probes of amyloid β aggregation†

Karna Terpstra,‡ Yiran Huang,‡ Hanah Na,  ‡ Liang Sun,‡ Citlali Gutierrez, 
Zhengxin Yu and Liviu M. Mirica *

The aggregation of amyloid β (A β) peptides is a significant hallmark of Alzheimer's disease (AD), and the detection of A β aggregates and the inhibition of their formation are important for the diagnosis and treatment of AD, respectively. Herein, we report a series of benzothiazole-based Ir(III) complexes **HN-1** to **HN-8** that exhibit appreciable inhibition of A β aggregation *in vitro* and in living cells. These Ir(III) complexes can induce a significant fluorescence increase when binding to A β fibrils and A β oligomers, while their measured log *D* values suggest these compounds could have enhanced blood–brain barrier (BBB) permeability. *In vivo* studies show that **HN-1**, **HN-2**, **HN-3**, and **HN-8** successfully penetrate the BBB and stain the amyloid plaques in AD mouse brains after a 10-day treatment, suggesting that these Ir(III) complexes could act as lead compounds for AD therapeutic and diagnostic agent development.

Received 10th June 2024,
Accepted 1st August 2024

DOI: 10.1039/d4dt01691b

rsc.li/dalton

Introduction

Alzheimer's disease (AD) is the most common neurodegenerative disease and the 7th leading cause of death in the US.¹ One strategy for the treatment of AD is the development of inhibitors that prevent the aggregation of monomeric A β peptides into neurotoxic A β species.^{2–12} Transition metal complexes have emerged as a viable alternative to organic compounds with distinct biological properties and have been widely utilized for the treatment of cancer.^{13,14} Recently, transition metal complexes have been developed as chemical reagents capable of altering A β aggregation.^{15–38} Among many of these transition metal complexes, cyclometalated Ir(III) complexes would be promising candidates as their photophysical and photochemical properties are unique and desirable. In general, these complexes exhibit high luminescence quantum yields and long lifetimes due to the efficient spin–orbit coupling induced by the heavy Ir(III) center. Also, they have high thermal and chemical stability, as Ir(III) is a substitutionally inert transition metal ion.^{39,40} Moreover, tuning the emission color and excited-state dynamics is easily achieved through ligand structure modification, by either increasing conjugation, introducing heteroatoms, and/or various substituents.

The preparation of Ir(III) complexes is highly modular when compared to the multi-step and linear synthesis of organic molecules.^{41,42} This synthetic versatility could be exploited to enhance the interaction of Ir(III) complexes with A β species, which could be employed for controlling the A β aggregation pathways.^{29,43,44}

In this work, eight Ir(III) complexes that contain A β -binding heterocycle ligands were designed and synthesized. These complexes with two or three A β binding groups are stable and exhibit optimal log *D* values and appreciable affinity for A β fibrils and A β oligomers. Importantly, *in vivo* studies have shown that four of the Ir(III) complexes specifically label the amyloid species in the brains of transgenic AD mice.

Results and discussion

Compounds design, synthesis and characterization of Ir(III) complexes

Complexes **HN-1** to **HN-3**, with 2-phenyl-1,3-benzothiazole as the 'C^N' ligand, were first designed and synthesized (Fig. 1, see ESI† for experimental details). **HN-1** is a cationic Ir(III) complex with two labile acetonitrile (MeCN) ancillary ligands, which allow for potential coordination to the A β amino acid residues. Then, **HN-2** was designed as a neutral tris-cyclometalated Ir(III) complex with increased lipophilicity and the potential to cross the blood–brain barrier (BBB). **HN-3** was also a neutral complex with an acetylacetonate (acac) ancillary ligand, which could be further modified. Complexes **HN-4** to **HN-6** were constructed by extension of the 2-phenyl-1,3-ben-

Department of Chemistry, University of Illinois at Urbana-Champaign, 600 S. Mathews Avenue, Urbana, Illinois 61801, USA. E-mail: mirica@illinois.edu

†Electronic supplementary information (ESI) available: Experimental section and Fig. S1–S30. CCDC 2070088. For ESI and crystallographic data in CIF or other electronic format see DOI: <https://doi.org/10.1039/d4dt01691b>

‡These authors contributed equally to this work.

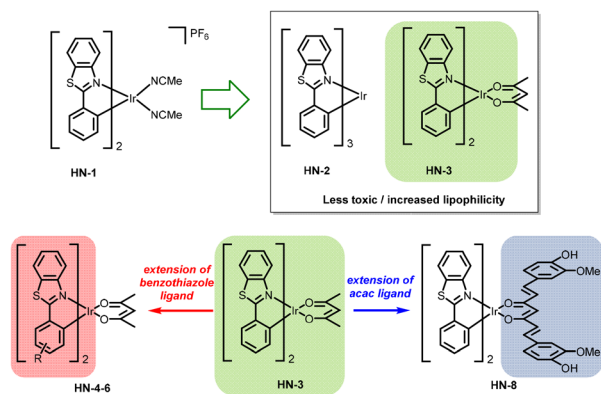
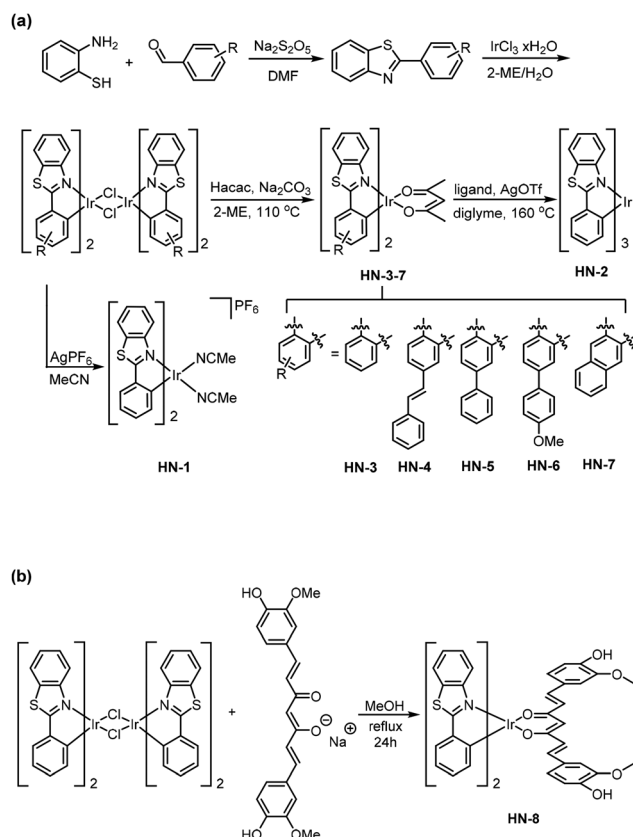


Fig. 1 Rational design strategies of Ir(III) complexes.

zothiazole C^N ligand with a pendant aromatic fragment. We proposed that the pendant moiety could rotate freely in solution, yet its free rotation would be hindered when the corresponding Ir(III) complexes would interact with the A β fibrils, and thus a fluorescence “turn-on” effect would be observed. Complex **HN-8** was designed by replacing the acac ligand with curcumin, a natural product which has been reported to have the ability to alleviate A β toxicity (Scheme 1).^{45–47} Importantly, replacing the acac ligand with other anionic che-



Scheme 1 Synthetic routes to Ir(III) complexes. (a) Complexes **HN-1–7**; (b) complex **HN-8**.

lating ligands is practical, since attaching the acac-related ligand is the last step in the synthesis of these inert Ir(III) complexes.

The molecular structure of **HN-1** was determined by single crystal X-ray diffraction (Fig. 2). The Ir atom adopts a distorted octahedral coordination geometry, with two C^N cyclometalated ligands and two acetonitrile ligands bound to the Ir center. The C^N nitrogen atoms are in a *trans* orientation relative to each other. The Ir–C and Ir–N bond lengths of **HN-1** are similar to those of the previously reported Ir(III) complexes with the 2-phenyl-1,3-benzothiazole C^N ligand, ranging between 2.007 and 2.143 Å.^{42,48,49}

Photophysical and biochemical properties of Ir(III) complexes

The UV-vis absorption spectra of **HN-1** to **HN-8** were obtained in PBS with 0.5% DMSO (Fig. S1[†]).⁵⁰ Complexes **HN-1**, **HN-2**, **HN-3**, and **HN-8** display intense absorption bands around 320 nm that can be assigned to spin-allowed ligand-centered $\pi-\pi^*$ transitions (¹LC). Due to the varied backbone C^N ligand for complexes **HN-4** to **HN-7**, the spin-allowed ligand-centered $\pi-\pi^*$ transitions (¹LC) occur around 370, 350, 355, and 335 nm, respectively. Less intense charge transfer (^{1,3}CT) absorption bands around 500 nm can be observed in the spectra for all eight complexes.

These complexes exhibit emission in the 520–700 nm region in PBS (Fig. 3a and Fig. S2[†]), where the Stokes shift is significantly large due to the phosphorescent properties of Ir(III) complexes.

As shown in Fig. 3a (black line), **HN-1** showed an excellent turn-on response toward the A β ₄₂ fibrils, displaying a nearly 200-fold fluorescence intensity increase ($\lambda_{em} = 550$ nm) for A β ₄₂ fibrils and with a K_i value of 3.6 ± 0.3 μ M (Fig. S7[†]).⁵⁰ This is likely due to the MeCN ligands in the Ir(III) complex being replaced by amino acid residues of the A β aggregates and therefore the Ir(III) complex coordinates to the peptides, as proposed previously.^{51,52}

In recent years, mounting evidence indicates that soluble A β oligomers are highly toxic for neurons.^{53,54} Therefore, Ir(III) complexes developed in this study were also tested to

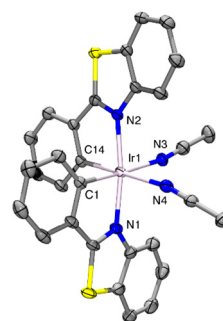


Fig. 2 X-ray crystal structure of **HN-1**. Thermal ellipsoids are drawn at the 50% probability with solvent molecules, counter ion and hydrogen atoms are eliminated for clarity. Selected bond distances (Å): Ir1–C1, 2.007(3); Ir1–C14, 2.008(3); Ir1–N1, 2.061(3); Ir1–N2, 2.064(3); Ir1–N3, 2.128(3); Ir1–N4, 2.143(3).

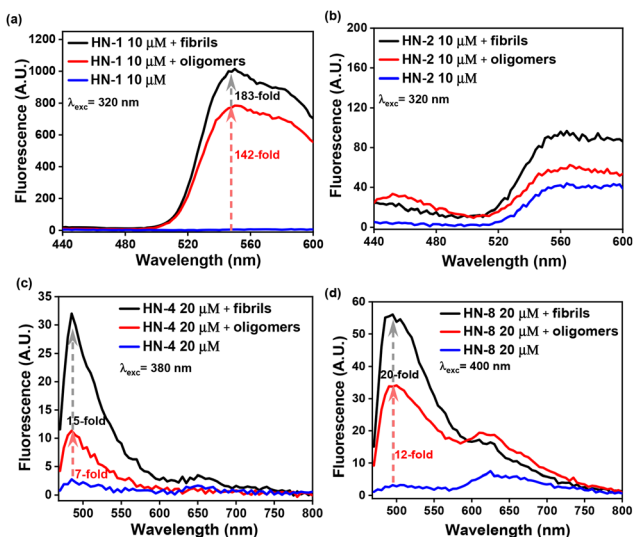


Fig. 3 Fluorescence spectra of Ir(III) complexes with or without A β_{42} fibrils (10 μ M) or A β_{42} oligomers (10 μ M). (a) HN-1, (b) HN-2, (c) HN-4, and (d) HN-8.

see whether they could interact with soluble A β_{42} oligomers. The A β_{42} oligomers were prepared according to the procedure reported by Klein *et al.*, and the morphology of obtained species was confirmed by transmission electron microscopy (TEM, Fig. S6 \dagger).⁵⁰ Surprisingly, **HN-1** also showed a nearly 150-fold fluorescence intensity increase with soluble A β_{42} oligomers (Fig. 3a, red line). Complexes **HN-2** (Fig. 3b) and **HN-3** did not exhibit a significant fluorescence increase when they bind to A β aggregates, which is also consistent with our previous assumption that the molecular structures of these complexes are too rigid. However, the K_i values of complexes **HN-2** and **HN-3** were similar to that of **HN-1** at 6.0 ± 1.9 and 7.7 ± 1.0 μ M, respectively (Fig. S7 \dagger), indicating they bind to A β fibrils with similar affinity due to interactions between the A β species and the 2-phenyl-benzothiazole ligand framework. As expected, the extended conjugated complexes **HN-4** and **HN-8** showed only slight turn-on effects when they bind to A β fibrils, with a 15-fold fluorescence increase for **HN-4** (Fig. 3c), and a 20-fold increase for **HN-8** (Fig. 3d), respectively.

Inhibition of amyloid β aggregation

The ability of the Ir(III) complexes to inhibit A β aggregation was probed *via* thioflavin T (ThT) fluorescence assays. ThT is a well-established fluorophore for the kinetic measurement of A β aggregation, and it is known that when it binds to amyloid fibrils, a pronounced enhancement of fluorescence can be detected at $\lambda_{\max} = 485$ nm upon excitation at 435 nm. The aggregation of A β follows a sigmoidal curve, composed of three phases: a lag phase, an elongation phase, and a plateau phase (Fig. 4, black line). Compared to the control group, Ir(III) complexes **HN-1** to **HN-7** exhibit the ability to modulate A β aggregation to different extents. Excitingly, **HN-1** comple-

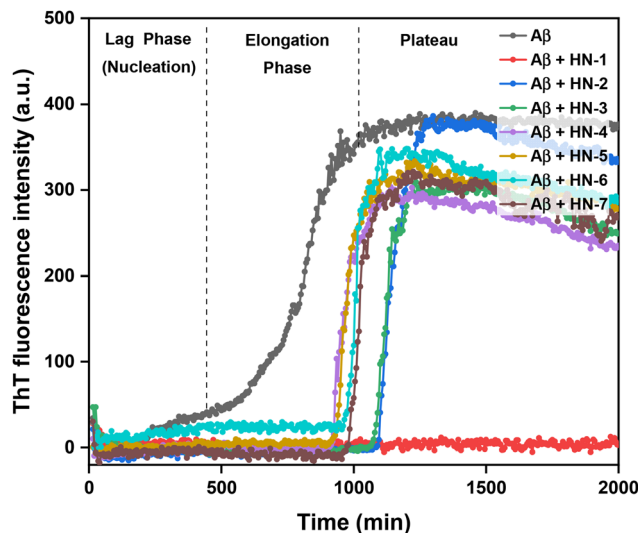


Fig. 4 Time-resolved measurements of the aggregation of A β_{42} through examination of ThT emission at 485 nm ($\lambda_{\text{ex}} = 435$ nm) for free A β_{42} and A β_{42} incubated with the ligands **HN-1** to **HN-7**. Conditions: [A β_{42}] = 10 μ M; [ThT] = 10 μ M; [compound] = 10 μ M.

tely quenched the A β aggregation (Fig. 4, red line, inhibition percentage: 100%), likely due to the replacement of acetonitrile ligands of **HN-1** with histidine residues located at the N-terminus region of A β peptide, which play critical role in A β aggregation.⁵⁵ The remaining Ir(III) complexes **HN-2** to **HN-7** extended the lag phase and delayed the beginning of the elongation phase. By comparison, **HN-8** exhibited a different behavior, likely due to the known decomposition of curcumin derivatives under physiological conditions (Fig. S10 \dagger). Importantly, we note that neither the excitation nor emission wavelengths of ThT overlap with those of the Ir(III) complexes.

5xFAD mouse brain section imaging

To examine whether the Ir(III) complexes could specifically interact with native A β species, brain section staining was performed. All brain sections were sliced from transgenic 5xFAD mice, which can overexpress human APP and PSEN1 transgenes. All of the eight Ir(III) complexes can specifically label A β plaques, showing excellent colocalization with staining of CF594 conjugated HJ3.4 antibody (CF594-HJ3.4) that binds to a wide range of A β species (Fig. 5).⁵⁶

log D measurements of Ir(III) complexes

The partition coefficients log D values were also examined to evaluate the BBB permeability of the Ir(III) complexes. For complexes **HN-2** to **HN-5**, **HN-7**, and **HN-8**, log D values in the range of 0.9–2.5 were obtained (Table 1), suggesting these compounds are promising candidates for further *in vivo* studies. In the case of the cationic complex **HN-1**, as expected, a lower log D was obtained. **HN-6** also showed a low log D value, presumably because of hydrogen bond formation through the methoxy group present on the ligand.

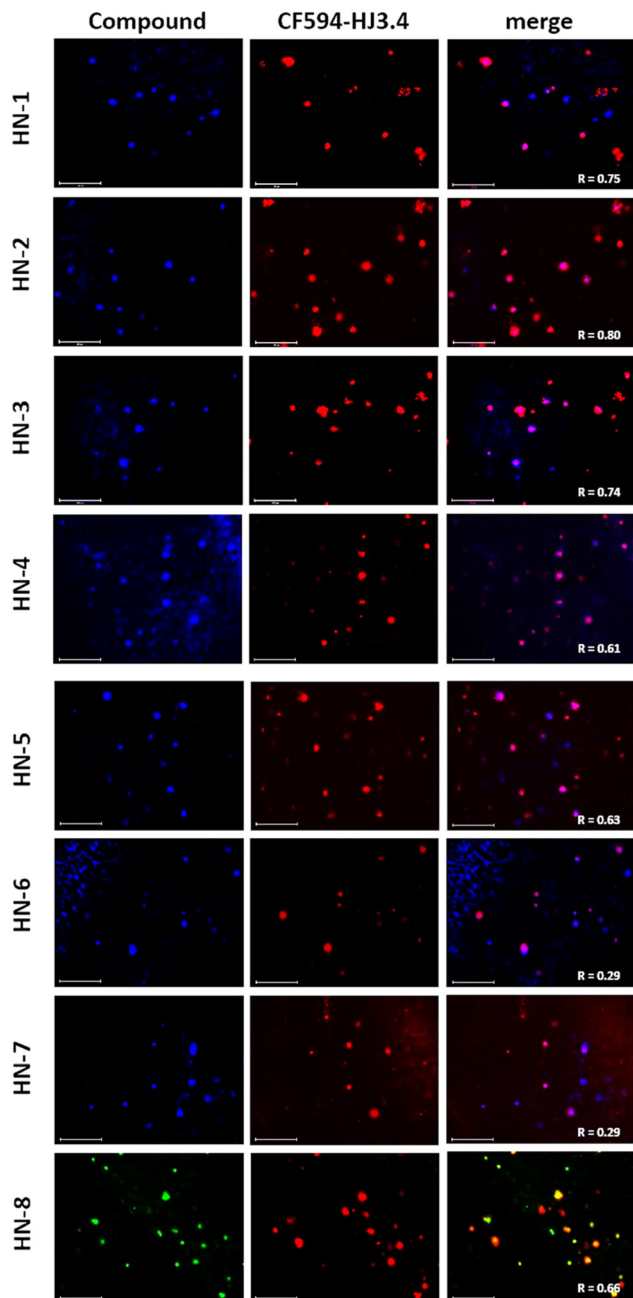


Fig. 5 Fluorescence microscopy images of 5xFAD mice brain sections incubated with Ir(III) complexes. The fluorescence signals from Ir(III) complexes and CF594-HJ3.4 antibody were monitored under blue and red channels, respectively. Scale bar: 125 μm . R = Pearson's correlation coefficient.

Table 1 Partition coefficients ($\log D$) of Ir(III) complexes in octanol/PBS

Iridium complex	$\log D$
HN-1	0.650 ± 0.110
HN-2	1.220 ± 0.055
HN-3	1.313 ± 0.067
HN-4	1.013 ± 0.084
HN-5	1.113 ± 0.029
HN-6	0.571 ± 0.028
HN-7	1.509 ± 0.020
HN-8	1.434 ± 0.047

Cytotoxicity of A β species upon incubation with Ir(III) complexes

The neurotoxicity of the Ir(III) complexes and their ability to alleviate the A β -induced neurotoxicity was investigated using mouse neuroblastoma N2a cells (American Type Culture Collection CCL-131TM). First, we examined the toxicity of all Ir(III) complexes at various concentrations ranging from 2 to 20 μM (Fig. 6a). Except for **HN-1**, all other iridium(III) complexes show very low cytotoxicity up to 20 μM . Then, the N2a cells were treated with A β_{42} in the absence or presence of the Ir(III) complexes to investigate whether the inhibition of A β_{42} aggregation can result in the rescue of A β_{42} neurotoxicity (Fig. 6b). Co-treatment with any of the eight Ir(III) complexes showed a significant rescue of A β -induced neurotoxicity. For comparison, the N2a cells were also treated with A β_{42} in the presence of curcumin, showing that curcumin dramatically increased the A β -induced cytotoxicity, instead of rescuing the cells (Fig. S11[†]).⁵⁰ Since curcumins are quite unstable in PBS and cell media,⁵⁷ the metabolites may promote A β -mediated cytotoxicity. However, in case of the curcumin-Ir(III) complex **HN-8**, the chelation between the metal center and the ligand could stabilize the curcumin structure or influence the mechanism of degradation, thus resulting in improved cell viability. Overall, the cell toxicity data reveals that Ir(III) complexes developed herein can efficiently decrease the A β -induced cyto-

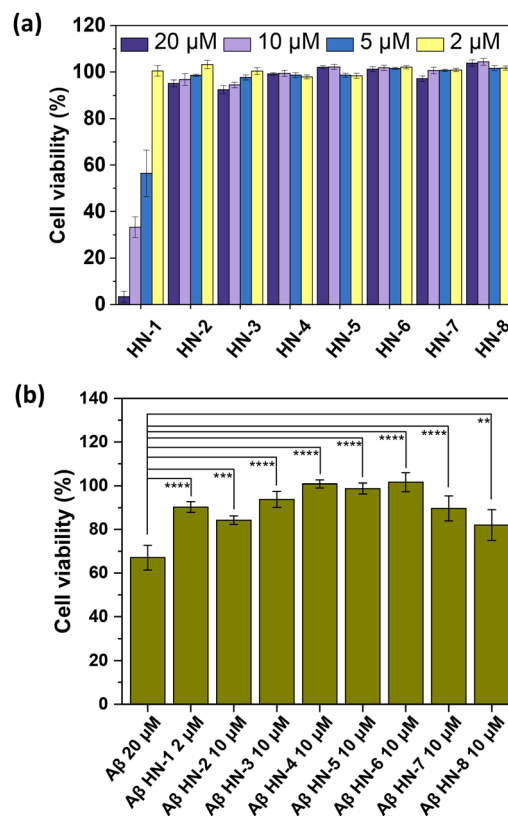


Fig. 6 (a) Cytotoxicity studies of Ir(III) complexes. (b) Cytotoxicity studies of Ir(III) complexes with A β_{42} .

toxicity in N2a cells, and thus can be employed in *in vivo* studies.

In vivo blood–brain barrier permeability

The BBB permeability of the metal complexes has significant implications for *in vivo* applications in AD research. Until recently, few metal complexes have shown the ability to cross the BBB without assistance.^{22,27,37,58,59} To evaluate the BBB permeability of the Ir(III) complexes, we have administered daily the Ir(III) complexes with the highest log *D* values, **HN-2**, **HN-3**, and **HN-8**, as well as the complex with the highest aqueous solubility, **HN-1**, to 11-month old 5xFAD mice at a dose of 1 mg kg⁻¹ of body weight *via* intraperitoneal injection for 10 days. Excitingly, upon brain extraction and analysis by fluorescence imaging of the resulting brain sections, all three complexes show appreciably accumulation in the 5xFAD mouse brains and fluorescence staining signals in both the DAPI and GFP channels for complexes **HN-2**, **HN-3**, and **HN-8** while **HN-1** exhibited signal only in the DAPI channel (Fig. S12†).⁵⁰ These fluorescence imaging studies demonstrate that the developed Ir(III) complexes can successfully cross the BBB, and the *in vivo* accumulated Ir(III) complexes have significant colocalization with the amyloid species that were subsequently immunostained with the HJ3.4 antibody (Fig. 7), confirming the specific binding of these Ir(III) complexes to the amyloid aggregates *in vivo*. Considering that the lower log *D*, more hydrophilic complex **HN-1**, as well as the higher

log *D*, more lipophilic complexes **HN-2**, **HN-3**, and **HN-8** exhibit BBB penetrability, these results lend promise to the development of optimal complexes that balance these two properties for improved BBB permeability.

Conclusions

Herein, a series of inert Ir(III) complexes **HN-1** to **HN-8** were designed and synthesized, and they exhibit appreciable A β inhibition ability *in vitro* and in living cells. A charged Ir(III) complex can induce a significant fluorescence increase upon binding to A β fibrils and A β oligomers, while neutral Ir(III) complexes induced a much smaller fluorescence increase despite similar affinity to fibrils. The measured log *D* values of the neutral complexes suggest these compounds have enhanced blood–brain barrier (BBB) permeability. Moreover, *in vivo* studies show that complexes **HN-1**, **HN-2**, **HN-3**, and **HN-8** successfully penetrate the BBB and stain the amyloid plaques in AD mouse brains after a 10-day treatment, suggesting that these Ir(III) complexes could act as lead compounds for AD therapeutic and diagnostic agent development. Further ligand design to optimize the aqueous solubility while maintaining the BBB permeability of such Ir(III) complexes may produce promising lead compounds with optimal drug-like characteristics.

Data availability

The data supporting this article have been included as part of the ESI.†

Crystallographic data for **HN-1** have been deposited at the Cambridge Crystallographic Data Centre (CCDC) under deposition numbers CCDC 2070088.†

Conflicts of interest

There are no conflicts to declare.

Acknowledgements

L. M. M. acknowledges research funding from the NIH (R01GM114588 and RF1AG083937).

References

- 1 *Alzheimer's Dementia*, 2023, **19**, 1598–1695.
- 2 S. Ayala, P. Genevoux, C. Hureau and P. Faller, *ACS Chem. Neurosci.*, 2019, **10**, 3366–3374.
- 3 J. Bieschke, J. Russ, R. P. Friedrich, D. E. Ehrnhoefer, H. Wobst, K. Neugebauer and E. E. Wanker, *Proc. Natl. Acad. Sci. U. S. A.*, 2010, **107**, 7710–7715.

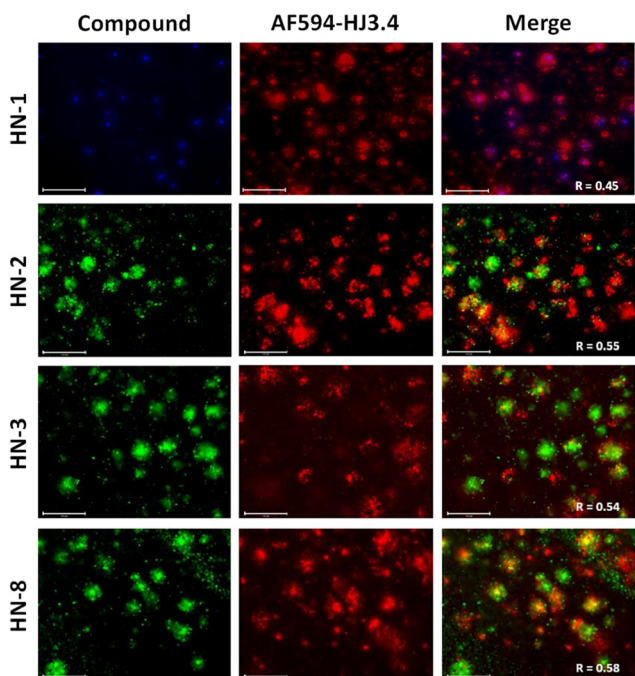


Fig. 7 Representative fluorescence microscopy images of brain sections from 11-month old 5xFAD mice administered with Ir(III) complexes for 10 days. The brain sections were subsequently immunostained with the HJ3.4 antibody ([HJ3.4] = 1 μ g ml⁻¹, scale bar = 125 μ m) with AF-594 fluorescent tag.

- 4 H.-J. Cho, A. K. Sharma, Y. Zhang, M. L. Gross and L. M. Mirica, *ACS Chem. Neurosci.*, 2020, **11**, 1471–1481.
- 5 L. M. F. Gomes, A. Mahammed, K. E. Prosser, J. R. Smith, M. A. Silverman, C. J. Walsby, Z. Gross and T. Storr, *Chem. Sci.*, 2019, **10**, 1634–1643.
- 6 Y. R. Huang, H. J. Cho, N. Bandara, L. Sun, D. Tran, B. E. Rogers and L. M. Mirica, *Chem. Sci.*, 2020, **11**, 7789–7799.
- 7 Y. Huang, L. Sun and L. M. Mirica, *Sens. Diagn.*, 2022, **1**, 709–713.
- 8 C. Rodríguez-Rodríguez, M. Telpoukhovskaia and C. Orvig, *Coord. Chem. Rev.*, 2012, **256**, 2308–2332.
- 9 M. G. Savelieff, G. Nam, J. Kang, H. J. Lee, M. Lee and M. H. Lim, *Chem. Rev.*, 2019, **119**, 1221–1322.
- 10 Z. Yu, Y. Moshood, M. K. Wozniak, S. Patel, K. Terpstra, D. A. Llano, L. W. Dobrucki and L. M. Mirica, *Chem. – Eur. J.*, 2023, **29**, e202302408.
- 11 Z. Yu, W. Guo, S. Patel, H.-J. Cho, L. Sun and L. M. Mirica, *Chem. Sci.*, 2022, **13**, 12818–12830.
- 12 H. J. Cho, T. T. Huynh, B. E. Rogers and L. M. Mirica, *Proc. Natl. Acad. Sci. U. S. A.*, 2020, **117**, 30928–30933.
- 13 P. Y. Ho, C. L. Ho and W. Y. Wong, *Coord. Chem. Rev.*, 2020, **413**, 213267.
- 14 A. Szczepaniak and J. Fichna, *Biomolecules*, 2019, **9**, 398.
- 15 A. Aliyan, N. P. Cook and A. A. Marti, *Chem. Rev.*, 2019, **119**, 11819–11856.
- 16 A. Aliyan, T. J. Paul, B. Jiang, C. Pennington, G. Sharma, R. Prabhakar and A. A. Martí, *Chem*, 2017, **3**, 898–912.
- 17 E. Babu, J. Bhuvaneshwari, K. Rajakumar, V. Sathish and P. Thanasekaran, *Coord. Chem. Rev.*, 2021, **428**, 213612.
- 18 K. J. Barnham, V. B. Kenche, G. D. Ciccotosto, D. P. Smith, D. J. Tew, X. Liu, K. Perez, G. A. Cranston, T. J. Johanssen, I. Volitakis, A. I. Bush, C. L. Masters, A. R. White, J. P. Smith, R. A. Cherny and R. Cappai, *Proc. Natl. Acad. Sci. U. S. A.*, 2008, **105**, 6813–6818.
- 19 J. C. Bataglioli, L. M. F. Gomes, C. Maunoir, J. R. Smith, H. D. Cole, J. McCain, T. Sainuddin, C. G. Cameron, S. A. McFarland and T. Storr, *Chem. Sci.*, 2021, **12**, 7510–7520.
- 20 J. S. Derrick, J. Lee, S. J. C. Lee, Y. Kim, E. Nam, H. Tak, J. Kang, M. Lee, S. H. Kim, K. Park, J. Cho and M. H. Lim, *J. Am. Chem. Soc.*, 2017, **139**, 2234–2244.
- 21 Z. Du, C. Liu, Z. Liu, H. Song, P. Scott, X. Du, J. Ren and X. Qu, *Chem. Sci.*, 2023, **14**, 506–513.
- 22 L. M. F. Gomes, J. C. Bataglioli and T. Storr, *Coord. Chem. Rev.*, 2020, **412**, 213255.
- 23 D. J. Hayne, S. Lim and P. S. Donnelly, *Chem. Soc. Rev.*, 2014, **43**, 6701–6715.
- 24 S. Jing, X. Wu, D. S.-H. Chan, S.-C. Nao, J. Du, C.-Y. Wong, J. Wang, C.-H. Leung and W. Wang, *Inorg. Chem. Front.*, 2024, **11**, 3400–3417.
- 25 J. Kang, S. J. C. Lee, J. S. Nam, H. J. Lee, M. G. Kang, K. J. Korshavn, H. T. Kim, J. Cho, A. Ramamoorthy, H. W. Rhee, T. H. Kwon and M. H. Lim, *Chem. – Eur. J.*, 2017, **23**, 1645–1653.
- 26 J. Kang, J. S. Nam, H. J. Lee, G. Nam, H. W. Rhee, T. H. Kwon and M. H. Lim, *Chem. Sci.*, 2019, **10**, 6855–6862.
- 27 V. B. Kenche, L. W. Hung, K. Perez, I. Volitakes, G. Ciccotosto, J. Kwok, N. Critch, N. Sherratt, M. Cortes, V. Lal, C. L. Masters, K. Murakami, R. Cappai, P. A. Adlard and K. J. Barnham, *Angew. Chem., Int. Ed.*, 2013, **52**, 3374–3378.
- 28 A. Kumar, L. Moody, J. F. Olaivar, N. A. Lewis, R. L. Khade, A. A. Holder, Y. Zhang and V. Rangachari, *ACS Chem. Neurosci.*, 2010, **1**, 691–701.
- 29 J. Kwak, J. Woo, S. Park and M. H. Lim, *J. Inorg. Biochem.*, 2023, **238**, 112053.
- 30 L. H. Lu, H. J. Zhong, M. D. Wang, S. L. Ho, H. W. Li, C. H. Leung and D. L. Ma, *Sci. Rep.*, 2015, **5**, 14619.
- 31 B. Y.-W. Man, H.-M. Chan, C.-H. Leung, D. S.-H. Chan, L.-P. Bai, Z.-H. Jiang, H.-W. Li and D.-L. Ma, *Chem. Sci.*, 2011, **2**, 917–921.
- 32 A. K. Sharma, S. T. Pavlova, J. Kim, D. Finkelstein, N. J. Hawco, N. P. Rath, J. Kim and L. M. Mirica, *J. Am. Chem. Soc.*, 2012, **134**, 6625–6636.
- 33 G. Son, B. I. Lee, Y. J. Chung and C. B. Park, *Acta Biomater.*, 2018, **67**, 147–155.
- 34 J. Suh, S. Yoo, M. Kim, K. Jeong, J. Y. Ahn, M. S. Kim, P. S. Chae, T. Y. Lee, J. Lee, J. Lee, Y. A. Jang and E. H. Ko, *Angew. Chem., Int. Ed.*, 2007, **46**, 7064–7067.
- 35 J. M. Suh, G. Kim, J. Kang and M. H. Lim, *Inorg. Chem.*, 2019, **58**, 8–17.
- 36 X. H. Wang, X. Y. Wang, C. L. Zhang, Y. Jiao and Z. J. Guo, *Chem. Sci.*, 2012, **3**, 1304–1312.
- 37 H. Y. Khan, A. Ahmad, M. N. Hassan, Y. H. Khan, F. Arjmand and R. H. Khan, *Coord. Chem. Rev.*, 2024, **501**, 215580.
- 38 G. S. Yellol, J. G. Yellol, V. B. Kenche, X. M. Liu, K. J. Barnham, A. Donaire, C. Janiak and J. Ruiz, *Inorg. Chem.*, 2015, **54**, 470–475.
- 39 L. Helm and A. E. Merbach, *Chem. Rev.*, 2005, **105**, 1923–1959.
- 40 M. S. Lowry and S. Bernhard, *Chem. – Eur. J.*, 2006, **12**, 7970–7977.
- 41 Y. Y. Zhou, H. F. Gao, X. M. Wang and H. L. Qi, *Inorg. Chem.*, 2015, **54**, 1446–1453.
- 42 R. J. Wang, D. Liu, H. C. Ren, T. Zhang, X. Z. Wang and J. Y. Li, *J. Mater. Chem.*, 2011, **21**, 15494–15500.
- 43 W. Wang, J. Liu, S.-C. Nao, D.-L. Ma, J. Wang and C.-H. Leung, *Inorganics*, 2022, **10**, 178.
- 44 G. S. Yellol, J. G. Yellol, V. B. Kenche, X. M. Liu, K. J. Barnham, A. Donaire, C. Janiak and J. Ruiz, *Inorg. Chem.*, 2015, **54**, 470–475.
- 45 M. Garcia-Alloza, L. A. Borrelli, A. Rozkalne, B. T. Hyman and B. J. Bacskaï, *J. Neurochem.*, 2007, **102**, 1095–1104.
- 46 F. Yang, G. P. Lim, A. N. Begum, O. J. Ubeda, M. R. Simmons, S. S. Ambegaokar, P. P. Chen, R. Kayed, C. G. Glabe, S. A. Frautschy and G. M. Cole, *J. Biol. Chem.*, 2005, **280**, 5892–5901.
- 47 Y. W. Zhao, J. D. Li, Z. Wu, H. Zhang, Y. F. Zhao, R. M. Yang and L. H. Lu, *Microchem. J.*, 2021, **160**, 105721.
- 48 Y. Q. Wu, H. Jing, Z. S. Dong, Q. Zhao, H. Z. Wu and F. Y. Li, *Inorg. Chem.*, 2011, **50**, 7412–7420.
- 49 H. Na, A. Maity and T. S. Teets, *Dalton Trans.*, 2017, **46**, 5008–5016.
- 50 A. Marchiani, S. Mammi, G. Siligardi, R. Hussain, I. Tessari, L. Bubacco, G. Delogu, D. Fabbri, M. A. Dettori,

- D. Sanna, S. Dedola, P. A. Serra and P. Ruzza, *Amino Acids*, 2013, **45**, 327–338.
- 51 D. L. Ma, W. L. Wong, W. H. Chung, F. Y. Chan, P. K. So, T. S. Lai, Z. Y. Zhou, Y. C. Leung and K. Y. Wong, *Angew. Chem., Int. Ed.*, 2008, **47**, 3735–3739.
- 52 X. C. Ma, J. L. Jia, R. Cao, X. B. Wang and H. Fei, *J. Am. Chem. Soc.*, 2014, **136**, 17734–17737.
- 53 I. Benilova, E. Karran and B. De Strooper, *Nat. Neurosci.*, 2012, **15**, 349–357.
- 54 J. P. Cleary, D. M. Walsh, J. J. Hofmeister, G. M. Shankar, M. A. Kuskowski, D. J. Selkoe and K. H. Ashe, *Nat. Neurosci.*, 2005, **8**, 79–84.
- 55 K. Brannstrom, T. Islam, L. Sandblad and A. Olofsson, *FEBS Lett.*, 2017, **591**, 1167–1175.
- 56 R. J. Perrin, A. M. Fagan and D. M. Holtzman, *Nature*, 2009, **461**, 916–922.
- 57 A. Marchiani, S. Mammi, G. Siligardi, R. Hussain, I. Tessari, L. Bubacco, G. Delogu, D. Fabbri, M. A. Dettori, D. Sanna, S. Dedola, P. A. Serra and P. Ruzza, *Amino Acids*, 2013, **45**, 327–338.
- 58 O. Krasnovskaya, D. Spector, A. Zlobin, K. Pavlov, P. Gorelkin, A. Erofeev, E. Beloglazkina and A. Majouga, *Int. J. Mol. Sci.*, 2020, **21**, 9190.
- 59 T. Storr, *Can. J. Chem.*, 2020, **99**, 1–9.